86, 41.
2. Baldacchini, G.; Pan, D. S.; Luty, F. *Phys. Rev. B.* **1981**, *24*, 2174.
3. Markham, J. J. In *F Centers in Alkali Halides*; Academic Press: New York, U.S.A., 1966; p 1.
4. De Matteis, F.; Leblans, M.; Joosen, W.; Schoemaker, D. *Phys. Rev. B.* **1992**, *45*, 10377.
5. Honda, S.; Tomura, M. *J. Phys. Soc. Jpn.* **1972**, *33*, 1003.
6. Bosi, L.; Bussolati, C.; Spinolo, G. *Phys. Rev. B.* **1970**, *1*, 890.
7. Dexter, D. L.; Klick, C. C.; Russell, G. A. *Phys. Rev.* **1955**, *100*, 603.
8. Gomes, L.; Morato, S. P. *J. Appl. Phys.* **1989**, *66*, 2754.
9. Bartram, R. H.; Stoneham, A. M. *Solid State Commun.* **1975**, *17*, 1593.
10. De Matteis, F.; Leblans, M.; Schoemaker, D. *Phys. Rev. B.* **1994**, *49*, 9357.
11. De Matteis, F.; Leblans, M.; Slootmans, W.; Schoemaker, D. *Phys. Rev. B.* **1994**, *50*, 13186.
12. Jang, D.-J.; Lee, J. *Solid State Commun.* **1995**, *94*, 539.
13. Casalboni, M.; Prosposito, P.; Grassano, U. M. *Solid State Commun.* **1993**, *87*, 305.
14. Jang, D.-J.; Corcoran, T. C.; El-Sayed, M. A.; Gomes, L.; Luty, F. In *Ultrafast Phenomena V*; Fleming, G. R.; Siegman, A. E., Ed.; Springer-Verlag: Berlin, 1986; p 280.
15. Gomes, L.; Luty, F. *Phys. Rev. B.* **1984**, *30*, 7194.
16. Yang, Y.; Luty, F. *Phys. Lett.* **1983**, *51*, 419.
17. Yang, Y.; von der Osten, W.; Luty, F. *Phys. Rev. B.* **1985**, *32*, 2724.
18. Halama, G.; Lin, S. H.; Tsen, K. T.; Luty, F.; Page, J. B. *Phys. Rev. B.* **1990**, *41*, 3136.
19. Tsen, K. T.; Halama, G.; Luty, F. *Phys. Rev. B.* **1987**, *36*, 9247.
20. Halama, G.; Tsen, K. T.; Lin, S. H.; Page, J. B. *Phys. Rev. B.* **1991**, *44*, 2040.
21. Cachei, G.; Stoltz, H.; van der Osten, W.; Luty, F. *J. Phys. Condens. Matter* **1989**, *1*, 3239.
22. Halama, G.; Tsen, K. T.; Lin, S. H.; Luty, F.; Page, J. B. *Phys. Rev. B.* **1989**, *39*, 13457.
23. Krantz, M.; Luty, F. *Phys. Rev. B.* **1988**, *37*, 8412.
24. Krantz, M.; Luty, F.; Dierolf, V.; Paus, H. *Phys. Rev. B.* **1991**, *43*, 9888.
25. Sothe, H.; Spaeth, J.-M.; Luty, F. *J. Phys. Condens. Matter* **1993**, *5*, 1957.
26. Jang, D.-J.; Kelley, D. F. *Rev. Sci. Instrum.* **1985**, *56*, 2205.
27. Luty, F. In *Physics of Color Centers*; Fowler, W. B., Ed.; Academic Press: New York, U.S.A., 1968; p 182.
28. Holstein, T.; Lyo, S. K.; Orbach, R. *Phys. Rev. B.* **1977**, *6*, 934.
29. Klein, M. V.; Wedding, B.; Levine, M. A. *Phys. Rev. B.* **1969**, *180*, 902.
30. Wedding, B.; Klein, M. V., *Phys. Rev.* **1969**, *177*, 1274.
31. Harrison, D. *Ph. D. Thesis*; Univ. of Utah: Salt Lake City, U.S.A., 1970; p 1.
32. Kapphan, S.; Luty, F. *Solid State Commun.* **1970**, *8*, 349.
33. Gomes, L.; Luty, F. In *Proceedings of the International Conference on Defects in Insulating Crystals*; Salt Lake City, U.S.A., 1984; p 182.
34. Narayananmurti, V.; Pohl, R. O. *Rev. Mod. Phys.* **1970**, *42*, 201.
35. Kapphan, S. *J. Phys. Chem. Solids* **1974**, *35*, 621.
36. Bridges, F. *CRC Crit. Rev. Solid State Sci.* **1975**, *5*, 1.
37. Baldacchini, G.; Botti, S.; Grassano, U. M.; Gomes, L.; Luty, F. *Europhys. Lett.* **1989**, *9*, 735.

Prediction of Lipophilicity of Orthopramides by Comparative Molecular Field Analysis (CoMFA)

Sung-eun Yoo* and Young Ah Shin

Korea Research Institute of Chemical Technology, Daedeog Science Complex, Taejon 305-606, Korea
Received August 18, 1995

The comparative molecular field analysis (CoMFA) method has been employed to correlate the apparent lipophilicity ($\log k_w$) and global lipophilicity ($\log P$) for orthopramide derivatives. This study demonstrated that CoMFA is an excellent method in predicting the complex properties of molecules such as apparent lipophilicity ($\log k_w$) or lipophilicity ($\log P$). The better predictability of lipophilicity by introducing $\log k_w$ as an independent descriptor suggests that the HPLC capacity factor measured in a buffer of pH 7.5 ($\log k_w$) can be effectively utilized in the prediction of global lipophilicity.

Introduction

Comparative Molecular Field Analysis (CoMFA),[1] a new 3-D QSAR (quantitative structure-activity relationship) approach developed by Cramer *et al.*, has become a popular and valuable tool in drug design.[2] Traditional QSAR attempts to correlate the biological properties of a series of molecules with the physicochemical property which are normally derived empirically. However, the CoMFA method tries to correlate the target variables with more fundamental properties of the molecules, steric and electrostatic properties. These properties are calculated theoretically and thus, CoMFA does not require predetermined physicochemical parameters for the analysis. Moreover, classical 2D-QSAR is applied only

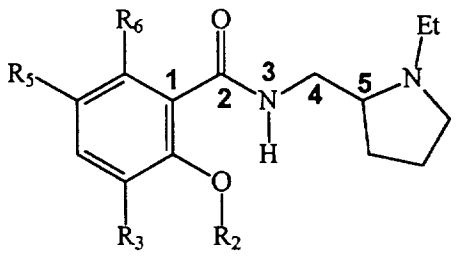

Figure 1. Chemical structure of general orthopramides.

to a congeneric series, but on the other hand CoMFA can be applied to mixed series. Recently, several studies have been reported in which the CoMFA method were used successfully to predict the classic QSAR descriptors such as Hammett constant,[3] pK_a,[4] and rate constant[5] as well as biological activity.[6]

As part of our continuing efforts to evaluate the usefulness of the CoMFA method in predicting physical properties of a molecule, we chose lipophilicity (log*P*) and apparent lipophilicity ($\log k_w$) for the CoMFA study. Lipophilicity is an important parameter to consider in medicinal chemistry since it plays an important role in determining, in many cases, bioavailability and intrinsic activity. A most commonly used descriptor for global lipophilicity (log*P*) of molecules has been the octanol-water partition coefficient measured experimentally by the shake-flask method.[7] Recently, as an alternative descriptor for lipophilicity, a capacity factor which is obtained from the reverse-phase HPLC experiment has been proposed.[8] This value usually correlates well with log*P* and is measurable in a wider range of lipophilicity than by the shake-flask method. Particularly, the HPLC capacity factor measured in a buffer of pH 7.5 is used to describe apparent lipophilicity ($\log k_w$).

In this study, we performed a CoMFA analysis on experimentally measured apparent lipophilicity ($\log k_w$) and global lipophilicity (log*P*) of orthopramides[9] to confirm how reasonably $\log k_w$ can be used to describe apparent lipophilicity and to demonstrate how effectively this new 3D-QSAR method can predict lipophilicity of molecules.

Methods

Starting geometries for 42 orthopramides (Figure 1 and Table 1) were generated by the BUILD option in SYBYL (version 6.0)[10] and the conformational study was carried out by the GRID SEARCH from the starting geometries. The charges were calculated by Gasteiger-Marsili's method.[11] The CoMFA analysis was performed by using the QSAR option in SYBYL. The lowest energy conformers of each compound were superimposed by the least-squares fitting of C1, C2, N3, C4, and C5 atoms. The steric and electrostatic potentials were generated by using an sp^3 C probe with +1 charge (C^+), an H probe with +1 charge (H^+), and a O.spc probe atom with −1 charge ($O.spc^-$). The O.spc represents a single point charge oxygen with the van der Waals radius of 1.7766 Å which is commonly used to create a special type of water molecule. The grid used in the CoMFA analysis has a lattice spacing of 2 Å in the cube of −20 Å to +20 Å along the *x*, *y*, and *z* axes. The steric, in terms of the van der Waals (6-12) interactions, and electrostatic, Coulombic with a 1/r distance-dependent dielectric, potential energy fields were calculated at each lattice intersection on a regularly-spaced region. A computationally efficient statistical algorithm, a partial least squares (PLS) analysis,[12] was used in conjugation with cross-validation[13] to measure the predictability of the dataset.

Table 1. Structures and Physicochemical Properties of Orthopramide Series[a]

	R_2	R_3	R_5	R_6	$\log k_w$	log*P*
1	Me	H	H	H	0.986	0.28
2	Me	H	Cl	H	1.852	–
3	Me	H	Br	H	1.979	–
4	Me	H	I	H	2.167	–
5	Me	H	OMe	H	1.124	0.56
6	Me	H	Et	H	1.832	1.64
7	Me	OMe	H	H	0.936	–
8	Me	OMe	Cl	H	1.697	–
9	Me	OMe	Br	H	1.818	–
10	Me	OMe	I	H	2.036	1.43
11	Me	OMe	Et	H	1.608	1.07
12	Me	OMe	Pr	H	2.102	–
13	Et	OMe	H	H	1.211	–
14	Et	OMe	Br	H	2.031	–
15	Et	OMe	I	H	2.182	–
16	Me	OEt	Br	H	2.395	–
17	Me	2-OEtF	Br	H	1.801	–
18	Me	OEt	I	H	2.339	2.32
19	Et	OEt	Br	H	2.467	–
20	Me	H	H	OH	1.629	–
21	Me	H	Br	OH	2.496	–
22	Me	H	I	OH	2.783	2.84
23	Me	H	OMe	OH	1.253	–
24	Me	H	Et	OH	2.805	–
25	Me	Cl	H	OH	2.044	–
26	Me	Cl	Cl	OH	2.681	2.76
27	Me	Cl	Br	OH	2.786	–
28	Me	Cl	I	OH	3.202	–
29	Me	Cl	Et	OH	3.323	–
30	Me	OMe	H	OH	1.460	0.94
31	Me	OMe	Cl	OH	1.920	–
32	Me	OMe	Br	OH	2.151	–
33	Me	OMe	I	OH	2.484	–
34	Me	OMe	Et	OH	2.507	2.14
35	Me	OMe	2-FEt	OH	2.074	–
36	Me	OMe	Pr	OH	3.083	–
37	Me	Br	Br	OH	2.741	–
38	Me	I	Br	OH	2.931	–
39	Me	I	Et	OH	3.585	–
40	Me	Br	OMe	OH	1.760	–
41	Me	I	OMe	OH	1.910	–
42	Me	Et	OMe	OH	1.718	–

[a] Ref. 9.

Table 2. CoMFA-PLS Analysis on Logk_w Values of 36 Orthopramides

	Model 1	Model 2	Model 3
probe atom	$C.3^+$	H^+	$O.spc^-$
cross-validated r^2	0.780	0.866	0.847
no-validated r^2	0.958	0.968	0.964
standard error (s)	0.140	0.122	0.130
no. of components	5	5	5
relative contribution			
steric	0.555	0.575	0.559
electrostatic	0.445	0.425	0.441

Table 3. Logk_w Values Predicted by Three CoMFA Models

	Expl.	Model 1	Model 2	Model 3
3	1.979	1.897	1.845	1.908
11	1.608	1.829	1.893	1.815
21	2.496	2.257	2.355	2.318
29	3.323	2.929	2.968	2.930
33	2.484	2.431	2.301	2.439
40	1.760	1.757	1.875	1.729
$S_{prediction}$		0.212	0.221	0.199

Results and Discussion

Correlation and prediction of apparent lipophilicity, logk_w. A CoMFA analysis of logk_w for the 36 orthopramide derivatives except for **3**, **11**, **21**, **29**, **33**, and **40** was carried out by using three different probe atoms. The CoMFA analysis as summarized in Table 2 shows a good correlation between the CoMFA interaction energy and the target property, logk_w. In all three models the cross-validated r^2 and no-validated r^2 values are high indicating that all three models are good in predicting logk_w of the orthopramide derivatives. As the next step to evaluate the predictability of the above models, we calculated the logk_w values for 6 omitted compounds, **3**, **11**, **21**, **29**, **33**, and **40**. The predicted values and the corresponding standard errors ($s_{prediction}$) are summarized in Table 3. The low standard error value, ~0.2, proves that the CoMFA models are very good in predicting the target values, logk_w. The plots of the calculated (squares) or predicted (triangles) logk_w values versus the observed ones show an excellent linearity as shown in Figure 2. The CoMFA contour maps for three models are similar regardless of the probe atom used and indicate that electropositive groups at the 3 and 5-position, electronegative groups at the 6-position, and sterically bulky groups at the 5-position of the benzene ring will increase logk_w of the orthopramide derivatives.

Correlation of lipophilicity, log*P*. The CoMFA analysis for ten compounds **1**, **5**, **6**, **10**, **11**, **18**, **22**, **26**, **30**, and **34** of which log*P* values are experimentally measured as listed in Table 1, was carried out using again three probe atoms. We also studied three additional models in which logk_w is used as an independent descriptor. The CoMFA analysis for log*P* as summarized in Table 4 again shows a good correlation with the CoMFA steric and electrostatic fields with high cross-validated r_2 and no-validated r^2 values. Particularly, the models 4, 5, and 6, where logk_w is introduced as an independent descriptor, show better predictabilities than the models 1, 2, and 3 in which only steric and electro-

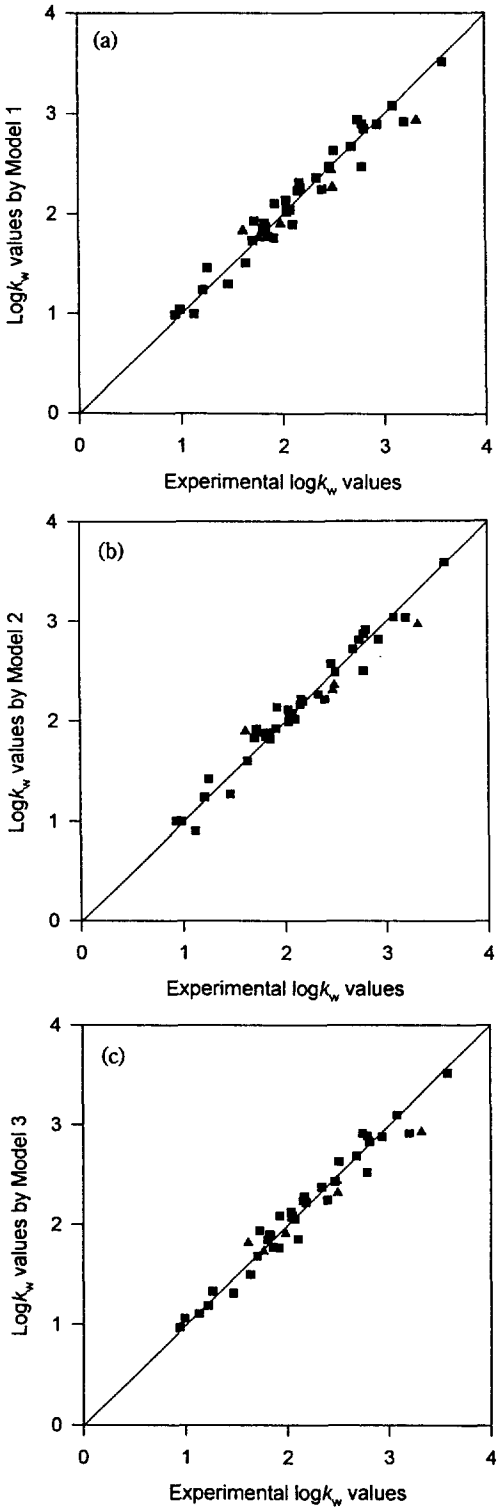

Figure 2. The plots of logk_w values calculated (squares) or predicted (triangles) by CoMFA models 1 (a), 2 (b), and 3 (c) versus experimental logk_w values.

Table 4. CoMFA-PLS Analysis on Log*P* Values of Ten Orthopramides

1	Model 2	Model 3	Model 4	Model 5	Model 6	Model
probe atom	$C.3^+$	H^+	$O.spc^-$	$C.3^+$	H^+	$O.spc^-$
descriptor	–	–	–	$\log k_w$	$\log k_w$	$\log k_w$
omitted compounds	**2**	**2**	**2**	–	–	–
cross-validated r^2	0.617	0.691	0.600	0.919	0.930	0.933
no-validated r^2	0.996	0.993	0.996	0.978	0.979	0.980
standard error (s)	0.086	0.120	0.086	0.150	0.146	0.146
no. of components	5	5	5	2	2	2
relative contribution						
$\log k_w$	–	–	–	0.787	0.769	0.782
steric	0.465	0.512	0.425	0.077	0.107	0.087
electrostatic	0.535	0.488	0.575	0.136	0.123	0.131

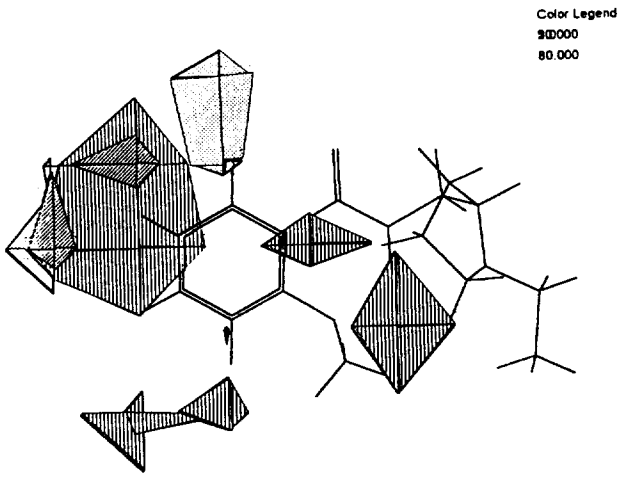

Figure 3. The CoMFA contour map for Model 1 for $\log k_w$. ▦, ▥, and ▨ are representing electronegative, electropositive, and sterically favored regions, respectively.

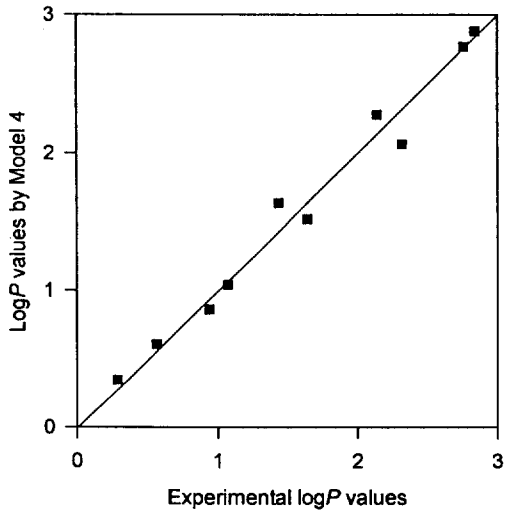

Figure 4. The plot of calculated log*P* values by Model 4 versus experimental values.

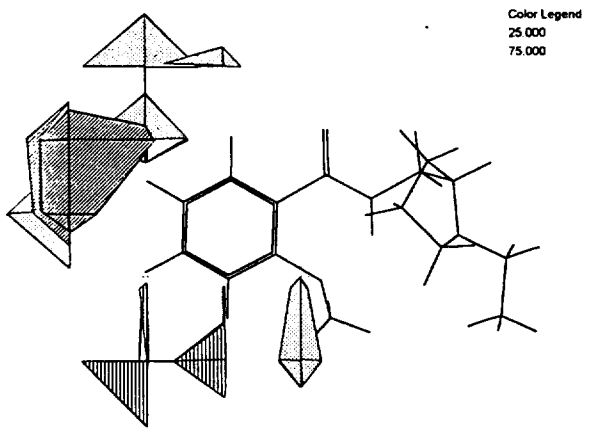

Figure 5. The CoMFA contour map for Model 4 for log*P* values. ▦, ▥, and ▨ are representing electronegative, electropositive, and sterically favored regions, respetively.

static fields are considered. The relative contribution by $\log k_w$ turns out to be very high, above 70%, suggesting that $\log k_w$ plays an important role in determining the log*P* values. Therefore, log*P* can be expressed as a linear function of $\log k_w$ as follow;

$$\log P = a \log k_w + b \quad (1)$$

for Model 4: $\log P = 1.325 \log k_w - 0.956$
for Model 5: $\log P = 1.307 \log k_w - 0.935$
for Model 6: $\log P = 1.327 \log k_w - 0.959$

A good linearity between $\log k_w$ and log*P* (Figure 4) suggests that $\log k_w$ can be usefully used for the prediction of log*P*. The contour map of this analysis (Figure 5) is similar to that of the $\log k_w$ analysis except no electropositive region at the 5-position of the phenyl ring. As shown in Figure 5, the CoMFA contour map for log*P* indicates that electropositive groups at the 3-position, electronegative groups at the 6-position, and sterically bulky groups at the 5-position of the benzene ring will increase log*P* of orthopramides.

Conclusion

In this work, we demonstrate that the CoMFA analysis can be usefully used for the prediction of log*P* of the orthopramide analogs. A good correlation of $\log k_w$ and log*P* with the CoMFA interaction energies regardless of probe atoms again indicates that lipophilicity can be predicted reasonably with only CoMFA analysis without using other descriptors, such as hydrogen-bonding factor, hydrophobic effect or other cross-interaction terms. Other clear advantage of the CoMFA method in the prediction of lipophilicity over the most of the log*P* prediction programs which normally can not differentiate regioisomers is that this method can differentiate regioisomers accordingly since this method treats any molecule as it is. A better predictability of lipophilicity by introducing $\log k_w$ as an independent descriptor in a linear function as $\log P = a \log k_w + b$ suggests that the HPLC capacity factor measured in a buffer of pH 7.5 ($\log k_w$) can be effectively utilized in the prediction of lipophilicity.

Acknowledgment. We thank Tripos Associates for

providing us the SYBYL® program.

References

1. Cramer III, R. D.; Patterson, D. E.; Bunce, J. D. *J. Am. Chem. Soc.* **1988**, *110*, 5959.
2. (a) Horwitz, J. P.; Massova, I.; Wiese, T. E.; Wozniak, A. J.; Corbett, T. H.; Sebolt-Leopold, J. S.; Capps, D. B.; Leopold, W. R. *J. Med. Chem.* **1993**, *36*, 3511. (b) Klebe, G.; Abraham, U. *J. Med. Chem.* **1993**, *36*, 70. (c) McFarland, J. W. *J. Med. Chem.* **1992**, *35*, 2543. (d) Kim, K. H. *Med. Chem. Res.* **1991**, *1*, 259.
3. Kim, K. H.; Martin, Y. C. *J. Org. Chem.* **1991**, *56*, 2723.
4. Kim, K. H.; Martin, Y. C. *J. Med. Chem.* **1991**, *34*, 2056.
5. Yoo, S. E.; Cha, O. J. *Bull. Korean Chem. Soc.* **1994**, *15*, 889.
6. (a) Carroll, F. I.; Gao, Y.; Rahman, M. A.; Abraham, P.; Parham, K.; Lewin, A. H.; Boja, J. W.; Kuhar, M. J. *J. Med. Chem.* **1991**, *34*, 2719. (b) Waller, C. L.; McKinney, J. D. *J. Med. Chem.* **1992**, *35*, 3660.
7. Rauls, D. O.; Baker, J. K. *J. Med. Chem.* **1979**, *22*, 81.
8. Altomare, C.; Tsai, R.-S.; Tayar, N. El; Testa, B.; Carroti, A.; Cellamare, S.; De Benedetti, P. G. *J. Pharm. Pharmacol.* **1991**, *43*, 191.
9. Dennis, E. S.; John, R. V.; Robert, M. K.; Tomas, De P. *J. Pharm. Sci.* **1994**, *83*, 305.
10. Tripos Associates, 1699 S. Hanley Road, Suite 303, St. Louis, MO 63144.
11. Gasteiger, J.; Marsili, M. *Tetrahedron* **1980**, *36*, 3219.
12. Wold, S.; Ruhe, A.; Wold, H.; Dunn, W. J. *SIAM J. Sci. Stat. Comp.* **1984**, *5*, 735.
13. Cramer, R. D.; Bunce, J. D.; Patterson, D. E.; Frank, I. E. *Quant. Struct.-Act. Relat.* **1988**, *7*, 18.

Analysis of Binodal Structures of Final State Distributions in Vibrational Predissociations of Triatomic van der Waals Molecules

Chun-Woo Lee

Department of Chemistry, Ajou University, 5 Wonchun Dong, Suwon 441-749, Korea
Received August 18, 1995

In this work, we focused on the setup of the tools for the analysis of the final rotational state distribution of photofragments in vibrational predissociations of triatomic van der Waals molecules A-B_2. We found that reflection principle used for the direct photodissociation processes can also be applied to find out the final rotational state distributions for indirect photodissociation processes. The quantity which represents the strength of rovibrational coupling between the quasi-bound state and the final state is reflected into the mirror of the classical angular momentum function, instead of the initial state before light absorption used in the reflection principle of direct processes. The sign change in the first derivative of the interaction potential with respect to the bond distance of B_2 is found to be the source of the binodal structures in the final rotational distributions of photofragments in the model system studied in this work. In MQDT analysis, short range eigenchannel basis functions were found to be localized in angle, in the previous work [Lee, C.W. *Bull. Korean Chem. Soc.* **1995**, *16*, 957.] and may be called angle functions. Angle functions enjoy simple geometrical structures which have simple functional relations with the final state distributions of photofragments. Two processes take place along the angle functions which resemble the quasi-bound state and dominate over other processes. Two such angle functions are found to be not only localized angularly but also localized either one of ends of B_2 in motions along the bond of B_2. These dominating photodissociation processes, however, cancel each other. This cancellation causes photodissociation to depend sensitively on the interaction potential at other angles than the dominant one. Part of potential surface where much larger torque exists can now play an important role in photodissociation. MQDT also enables us to see which processes play important roles after cancellation. This is done by examining the amounts of time delayed by asymptotic eigenchannels.

Introduction

It is a fundamental question in chemistry how and how fast the energies deposited into molecules by lights or by collisions redistribute inside the molecules and break up chemical bonds. The investigation of such nonradiative decay processes of excited states for medium-sized molecules is, however, greatly hampered by the presence of a lot of vibrotational or electronic channels involved. It has been recognized that van der Waals molecules provide the tractable system for state-to-state studies of intramolecular energy redistributions.[1] Van der Waals bonds are so weak that even one quantum excitation of vibration motion is in many cases enough to break down the bond without exciting electronic states. Consequently the number of channels involved are greatly reduced in the predissociation of van der Waals mol-